THE JOURNAL OF PHYSICAL CHEMISTRY C

Article

pubs.acs.org/JPCC

Electronic Structure of Diamond Surfaces Functionalized by $Ru(tpy)_2$

Ioannis Zegkinoglou,[†,‡] Peter L. Cook,[†,▽] Phillip S. Johnson,[†] Wanli Yang,[‡] Jinghua Guo,[‡] David Pickup,[§,⊥] Rubén González-Moreno,[§,#] Celia Rogero,[§,#] Rose E. Ruther,[∥] Matthew L. Rigsby,[∥] J. Enrique Ortega,[§,⊥,#] Robert J. Hamers,[∥] and F. J. Himpsel*[,†]

[†]Department of Physics, University of Wisconsin Madison, Madison, Wisconsin 53706, United States

[‡]Advanced Light Source, Lawrence Berkeley National Laboratory, Berkeley, California 94720, United States

[§]Material Physics Center (MPC), Centro de Física de Materiales (CSIC-UPV/EHU), 20018, San Sebastian, Spain

[∥]Department of Chemistry, University of Wisconsin Madison, Madison, Wisconsin 53706, United States

[⊥]Departamento de Fisica Aplicada I, Universidad del Pais Vasco, 20018, San Sebastian, Spain

[#]Donostia International Physics Center, 20018, San Sebastian, Spain

ABSTRACT: Highly doped diamond films are new candidates for electrodes in reactive environments, such as electrocatalytic interfaces. Here the electronic structure of such films is investigated by X-ray absorption spectroscopy at the C 1s and B 1s edges, combined with X-ray and ultraviolet photoelectron spectroscopy, as well as optical measurements. A diamond surface functionalized covalently with $Ru(tpy)_2$, a model complex similar to ruthenium-based molecules used in photocatalysis and photovoltaics, is compared to a hydrogen-terminated diamond surface as a reference. Bulk-sensitive absorption spectra with photon detection reveal diamond gap states, while surface-sensitive spectra with electron detection reveal the adsorbate states and π-bonding at the diamond surface. The positions of the frontier orbitals of the dye relative to the band edges of diamond are inferred from the spectroscopic data. The implications of using diamond films as inert electron donors in photocatalysis and dye-sensitized solar cells are discussed.

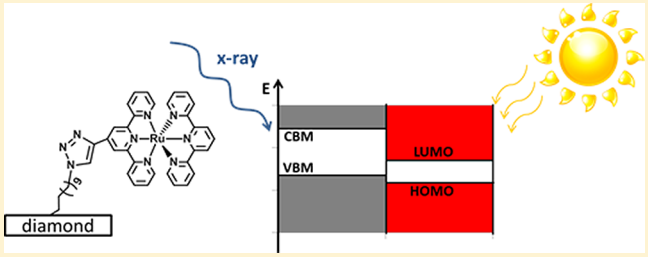

INTRODUCTION

For electrocatalysis in reactive environments, such as those present in solar energy conversion processes, it is important to attach electrochemically active molecules to the surface of inert electrodes and control the energy levels of their orbitals. A significant problem is the corrosion of the electrodes at potentials higher than 1 V, which are common in these processes. Recently it has been shown that polycrystalline synthetic diamond electrodes can mitigate the corrosion problem by remaining stable up to strongly oxidizing potentials.[1] In cyclic voltammetry experiments minimal corrosion of such electrodes is observed even after 1 million cycles at potentials as high as 1.5 V versus a normal hydrogen electrode (NHE) in nonaqueous electrolytes, while only a small decrease in their stability occurs in aqueous electrolyte solutions. Furthermore they are conductive, can be easily doped p-type by boron, are nontoxic, and can be produced at low cost by decomposition of hydrocarbon molecules. The downside of the low reactivity of diamond is the difficulty of attaching any kind of organic molecules to its surface. The difficulty can be overcome by using a photochemical attachment technique which allows for a variety of different functionalities to be introduced to the diamond surface.[2,3] Most recently a robust, covalent linking of ruthenium-based molecular complexes to the diamond surface has been demonstrated.[1]

This could open the door for employing dye-sensitized diamond surfaces in solar-driven water splitting (artificial photosynthesis), replacing expensive but widely used platinum catalysts. In dye-sensitized solar cells (DSSCs) p-doped diamond electrodes might be employed as electron donors to replace the traditional, highly corrosive tri-iodide electrolyte. Although tri-iodide fills the hole very rapidly and thereby prevents recombination, it does so by reducing the output voltage by almost a factor of 2.[4]

For all solar energy conversion processes, the relative energy positions of the frontier orbitals of light absorber, donor, and acceptor are crucial. These can be probed systematically by spectroscopic techniques.[5] Here we employ a combination of near-edge X-ray absorption fine structure (NEXAFS) spectroscopy with X-ray and ultraviolet photoelectron spectroscopy (XPS and UPS, probing core and valence levels, respectively). Together with ultraviolet/visible (UV−vis) spectroscopy these are used to investigate the electronic structure of $Ru(tpy)_2$-sensitized diamond surfaces (tpy = 2,2′:6′,2″-terpyridine).

Received: April 25, 2012
Revised: May 30, 2012
Published: June 11, 2012

dx.doi.org/10.1021/jp304016t | J. Phys. Chem. C 2012, 116, 13877−13883

Hydrogen-passivated diamond is used as a reference. The energies of the lowest unoccupied molecular orbital (LUMO) and highest occupied molecular orbital (HOMO) of the $Ru(tpy)_2$ dye are determined relative to the band edges of diamond, both in a bulk-like thin film and in a submonolayer attached to the diamond surface. Based on the relative position of the HOMO of the dye with respect to the valence band maximum (VBM) of diamond, the possibility of employing $Ru(tpy)_2$-sensitized diamond surfaces as electron donors in DSSCs is discussed. The gap states introduced in diamond by boron doping are detected at both the C 1s and B 1s edges. The combined use of bulk-sensitive fluorescence detection and surface-sensitive electron detection in NEXAFS reveals dramatic differences between bulk and surface. The results open up new territory in solar energy research by demonstrating the suitability of inert diamond thin films as electron donor electrodes in dye-sensitized solar cells and solar water splitting.

EXPERIMENTAL METHODS

NEXAFS spectroscopy investigations at the *K* edges of carbon and boron were conducted at Beamline 8.0.1 of the Advanced Light Source (ALS) at Lawrence Berkeley National Laboratory and at the VLS−PGM beamline of the Synchrotron Radiation Center (SRC) in Madison. The energy resolution was 0.1−0.2 eV at both edges. The photon energy was calibrated at the B 1s edge using as a reference the energy of the π^* absorption peak of bulk B_2O_3 powder (194.0 eV)[6−8] and at the C 1s edge using the energy of the π-peak of graphite (285.35 eV[9]). The total electron yield (TEY) and total fluorescence yield (TFY) data were collected simultaneously at ALS. For an efficient collection of the fluorescence yield, a channel plate detector with an Al filter was used. All absorption spectra were normalized to the incident photon flux. To do so, the NEXAFS intensities were divided by the current from a mesh coated in situ with Au, located in the X-ray beam path close to the sample position. All presented data were interpolated with a cubic spline function, with the pre-edge background set to zero.

Complementary XPS data were collected in the Chemistry Department of the University of Wisconsin (UW) in Madison. The data were obtained using a custom-built XPS system (Physical Electronics Inc.). Measurements were performed using an electron takeoff angle of 45° and an analyzer pass energy of 59 eV, yielding an analyzer resolution of 0.9 eV.

UPS studies were performed using the Apple PGM beamline combined with a Scienta 200U photoelectron spectrometer at the SRC and an in-house He(I) resonance lamp, both with overall energy resolution of better than 0.1 eV. The synchrotron measurements were performed at photon energies ranging from 20 to 50 eV. Energies were referenced to the Fermi level, which was determined by measuring the Fermi edge of a gold sample.

For the UV−vis investigation, a dilute solution of the $Ru(tpy)_2$ complex in acetonitrile was studied using a double beam Shimadzu UV−visible spectrophotometer and referenced to pure acetonitrile.

Synthetic, polycrystalline diamond substrates grown by chemical vapor deposition (CVD) were obtained from Element Six Ltd. They were heavily boron-doped with a concentration of at least 10^{20} cm^{-3} (570 ppm). At this doping level, diamond is close to becoming metallic.[10] The undoped diamond sample was an optically transparent, electronic-grade plate with polished surfaces.

Before spectroscopic investigation, all surfaces were cleaned in acid baths and then terminated with hydrogen by exposure to a hydrogen plasma (50 Torr H_2), as described elsewhere.[3] The hydrogen termination of diamond surfaces is known to reduce the energy barrier for electron emission by lowering the electron affinity.[11−15]

The synthesis of $Ru(tpy)_2$ and its covalent attachment to diamond surfaces are described in a previous publication.[1]

RESULTS AND DISCUSSION

X-ray absorption spectra at the C 1s edge of a boron-doped, hydrogen-terminated diamond are shown in Figure 1. These were measured using simultaneous detection of TEY and TFY. The bulk-sensitive TFY data exhibit a narrow, well-defined core exciton peak at energy 289.1 eV, in accordance with previous reports.[16−20] Taking into consideration that the binding energy of the core exciton in diamond is about 0.2 eV,[16] the conduction band minimum (CBM) is estimated to lie 0.2 eV higher than the exciton peak, that is, at 289.3 eV. Besides the excitonic peak, the TFY spectrum exhibits distinct peaks at energies 282.5 and 284.0 eV. These features, which will be referred to as "A" and "B", are due to the introduction of unoccupied states in the band gap of diamond by the boron dopant. This is verified in Figure 2 by comparison with the TFY spectrum of an undoped, H-terminated diamond sample. Peaks A and B are highly attenuated there. The absence of any graphitic π^* peak near 285.5 eV demonstrates that all carbon atoms in the bulk are in tetrahedral sp^3 coordination. The characteristic sharp exciton peak at 289.1 eV becomes broader and less intense upon doping, indicating the formation of defects near B dopants.

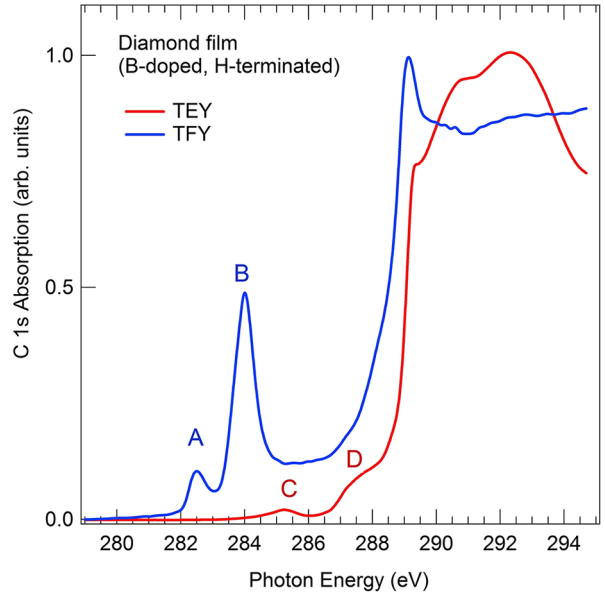

Figure 1. Comparison of bulk- and surface-sensitive C 1s absorption spectra of a B-doped, H-terminated diamond film obtained by detecting the total fluorescence yield (TFY) and total electron yield (TEY). The bulk-sensitive spectrum shows empty boron impurity states in the band gap at 282.5 (A) and 284.0 eV (B) and the C 1s core exciton at 289.1 eV. The surface-sensitive spectrum shows a different set of gap states at 285.3 (C) and 287.4 eV (D), which are assigned to π-bonded carbon and C−H monohydrides, respectively.

dx.doi.org/10.1021/jp304016t | J. Phys. Chem. C 2012, 116, 13877−13883

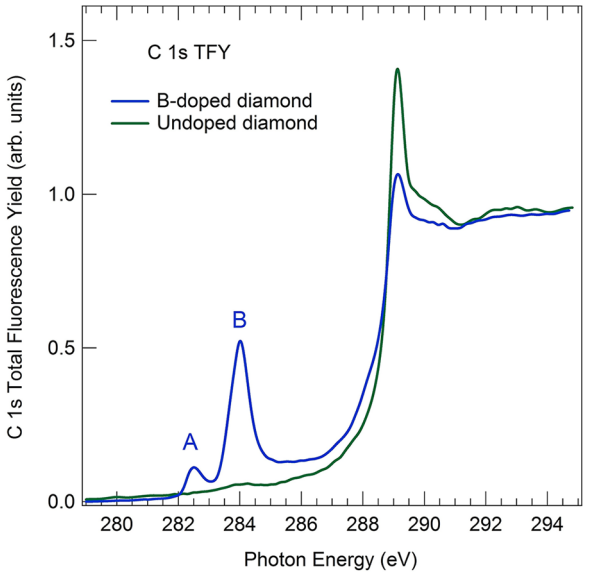

Figure 2. Comparison of B-doped and undoped diamond terminated with H. Bulk-sensitive C 1s absorption spectra in the fluorescence detection mode show that the empty states A and B in the band gap are only present in the B-doped diamond.

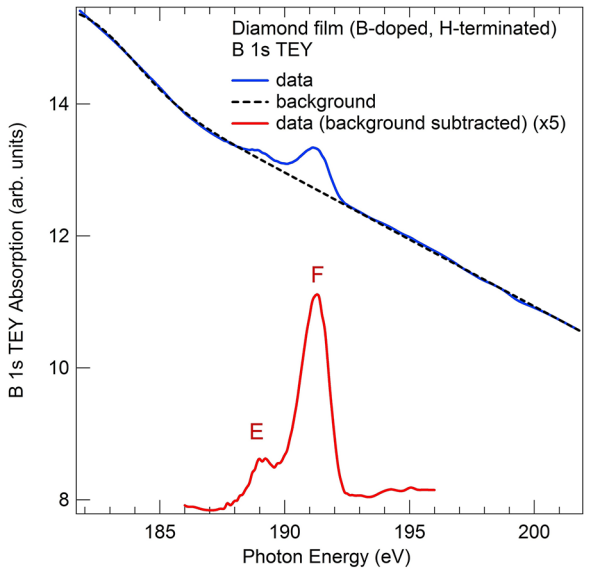

Figure 3. Empty impurity states due to the boron complexes at the surface of B-doped, H-terminated diamond. The sloping background is from valence absorption. It has been subtracted in the lower part of the panel.

In contrast to the TFY data, the two gap states are completely absent in the surface-sensitive TEY spectrum of Figure 1. Instead, two small features appear at 285.3 and 287.4 eV (labeled C and D). Peak C is assigned to π-bonded carbon and shoulder D to C−H monohydride at the surface, as will be discussed in the following. The excitonic peak is still present, but much less prominent than in the bulk-sensitive spectrum. This confirms the partial conversion from sp^3- to sp^2-bonded C at the surface. Repeated cleaning cycles with activated H reduce the π-bonded gap states and improve the sharpness and height of the sp^3-bonded exciton peak.

Complementary information about the boron-induced nature of the gap states is provided by similar NEXAFS data taken at the B 1s edge. The B 1s TEY spectrum of the boron-doped sample is shown in Figure 3. Despite the presence of a strong sloping background, originating from valence absorption, a double-peak structure can be clearly seen around 190 eV. The net B 1s absorption after subtraction of the background shows two peaks at 191.2 and 189.2 eV (labeled E and F). These are absent for undoped diamond (not shown), confirming the connection of peaks E and F to B doping.

Figure 4 combines NEXAFS data at the C 1s and B 1s edges from B-doped, H-terminated diamond. The position of the Fermi level, the CBM and the VBM are indicated by dotted lines. The CBM is obtained from the energy of the C 1s core exciton peak (289.1 eV in the TFY data) by adding the binding energy of the core exciton (0.2 eV[16]). For determining the position of the VBM (283.8 eV), the band gap of diamond (5.47 eV[12,21,22]) is subtracted from the CBM (289.3 eV). To allow direct comparison of the C 1s and B 1s absorption spectra in Figure 4, the difference of 96.9 eV between the C 1s and B 1s binding energies from XPS is used to shift the energy scales between the C 1s and B 1s NEXAFS spectra.

The position of the Fermi level E_F in the gap differs between the bulk (where it is determined by doping) and the surface (where it is determined by surface defect states). This leads to band bending accompanied by a substantial Schottky barrier in diamond. E_F (surface) in Figure 4b at 285.0 eV is the C 1s binding energy with respect to the Fermi level obtained by surface-sensitive XPS. It is 1.2 eV above the VBM. A similar E_F-VBM value of 1.4 eV is obtained by linear extrapolation of the UPS valence band edge (see Figure 6a). Previous studies investigated the energy difference E_F-VBM in diamond as a function of the dopant concentration, the surface treatment, and the crystallographic orientation of the surface. While E_F-VBM is only 0.25 eV in the bulk of B-doped diamond (at a concentration of 10^{20} cm^{-3}), it increases to 0.7 eV at the (1 0 0) surface of a H-terminated sample with the same B concentration, and it becomes as high as 1.6 eV at a clean (nonterminated) surface.[23−25] E_F-VBM is about 0.2 eV lower for (1 1 1) oriented surfaces. The value of 1.2 eV in our work is consistent with these studies, lying between the two extreme, previously reported surface values. The fact that it is higher than 0.7 eV may indicate that high B concentration leads to an incomplete H coverage of the surface. The bulk Fermi level of 0.25 eV above VBM, from refs 23 and 24, is shown for comparison in Figure 4a, together with the bulk-sensitive C 1s TFY data.

The substitutional boron acceptors introduced in modest concentrations to diamond by doping are known to introduce energy levels 0.37 eV above its VBM.[26] This matches the energy of the dominant peak B in Figure 4a, at 0.2 eV above the VBM, within the accuracy in determining the VBM via the core exciton. The weaker peak A lies 1.5 eV lower in energy. Peak A can be assigned to transitions into the same boron acceptor level from carbon atoms adjacent to boron, whose C 1s level is shifted to lower binding energy as a result of charge transfer from the more electropositive B. The energy difference between the two peaks corresponds to the chemical shift of the C 1s level. Such a core shift has been proposed in the literature and modeled using the discrete variational DV-X_α MO calculation method.[27,28] The core level energy difference of 1.5 eV is also very close to the value of 1.3 eV estimated by first-principles calculations for heavily doped diamond.[29]

The weaker gap features in the surface-sensitive TEY spectra of Figure 4b are located much higher in the gap than the bulk

dx.doi.org/10.1021/jp304016t | J. Phys. Chem. C 2012, 116, 13877−13883

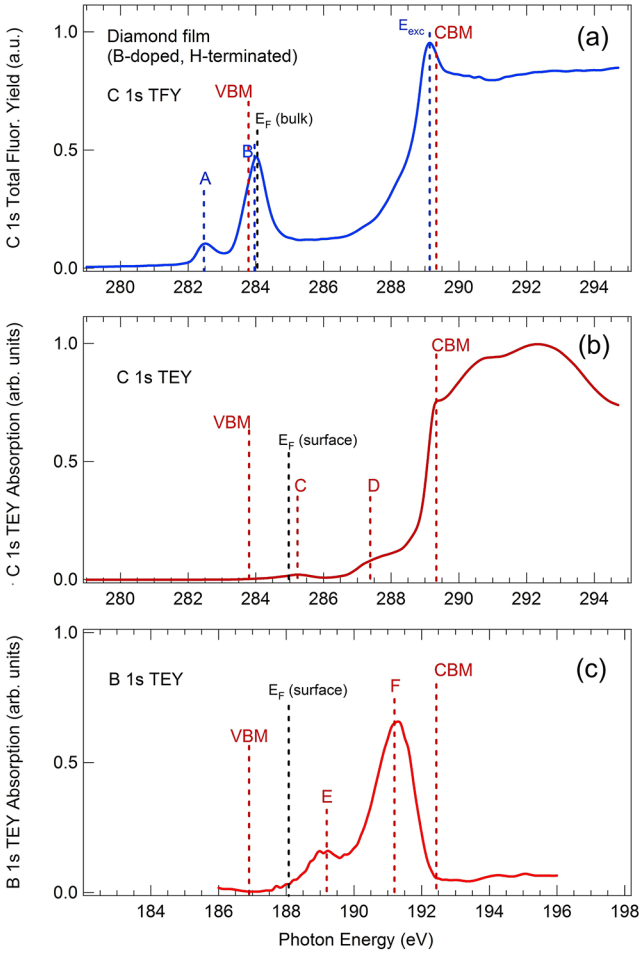

Figure 4. Comparison between the gap states measured at the C 1s and B 1s edges. The energy scales have been shifted by the difference of 96.9 eV between the C 1s and B 1s core levels as obtained from XPS. Thereby all spectra are referenced to the surface Fermi level (vertical dashed lines at 285.0 and 188.1 eV). The bulk Fermi level is shown with the bulk-sensitive TFY data in part a. The conduction band minimum (CBM) lies 0.2 eV above the C 1s core exciton and the valence band maximum (VBM) 5.47 eV below the CBM. That puts the dominant gap state (B) at 0.2 eV above the VBM and close to the boron acceptor level.

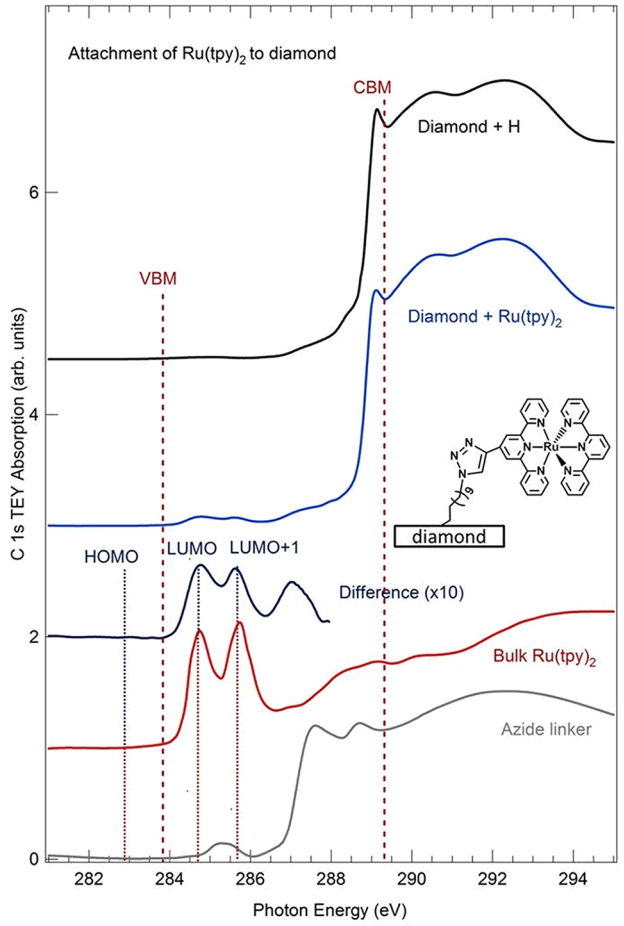

Figure 5. C 1s absorption spectra of diamond with Ru(tpy)$_2$ dye molecules tethered to its surface via an azide linker and an alkane chain (inset). Two π^* peaks of the dye are observed in the gap, which are absent for H-terminated diamond and the azide linker. Their positions provide a lower limit for the LUMO and LUMO+1, since the Coulomb interaction between the excited electron and the C 1s core hole reduces the excitation energy. The HOMO of the dye from Figure 6 lies below the VBM, as required for diamond acting as a donor. It needs to move closer to the VBM to minimize the voltage loss.

gap states, indicating a different origin. The feature at 285.3 eV (C) has been assigned previously to transitions into π^* states of sp^2-bonded C at the surface, while the feature at 287.4 eV (D) has been assigned to transitions into σ^* states of hydrocarbons, particularly of C−H monohydride.[30−32] The assignment of peak C to empty defect states is supported by the observation that it becomes weaker upon successive hydrogen treatments, while the exciton peak becomes sharper and stronger. This is clearly seen by comparing the TEY spectrum of the H-terminated sample in Figure 5 (which has undergone more frequent H treatments) to the TEY spectrum of the sample shown in Figures 1 and 4b.

Similarly to the C 1s TEY spectrum, the B 1s TEY spectrum shown in Figure 4c is also dominated by features originating from surface defects. The strongest peak at 191.2 eV (F) is likely due to the presence of boron−carbon complexes, such as B_4C, at the surface. Electronic transitions from the B 1s to the B 2p π^* states of B_4C are known to give rise to an absorption peak around 191.2 eV.[7] The weaker peak at 189.2 eV (E) has been tentatively assigned to empty states introduced by boron−hydrogen complexes.[33] Previous fluorescence yield measurements detected a sharp peak at 185 eV at the B 1s edge, which was assigned to transitions into the boron acceptor level.[27,33,34] This peak does not show up in our B 1s TEY spectra. That is in line with the observations at the C 1s edge, where the acceptor level is visible only in the bulk-sensitive TFY spectra, not in the surface-sensitive TEY spectra. Our TFY spectrum at the B 1s edge does not provide usable information because of a large background from C 1s emission induced by higher orders of the monochromator and the undulator.

The attachment of Ru(tpy)$_2$ dye molecules to the diamond surface is characterized in Figure 5 by a series of C 1s spectra, all taken in the surface-sensitive TEY mode. The top spectrum from H-terminated diamond is compared to the spectrum below it, which is from a submonolayer of Ru(tpy)$_2$ dye attached covalently to H-terminated diamond (inset). The difference spectrum exhibits several features appearing in the gap (after amplification by a factor of 10). To correlate these features with the attached dye molecules, a spectrum of bulk

dx.doi.org/10.1021/jp304016t | J. Phys. Chem. C 2012, 116, 13877−13883

$Ru(tpy)_2$ is shown below the difference curve. This was obtained from a drop of a dye solution in acetonitrile, dried on gold. The bulk and monolayer spectra are both dominated by π^* peaks at energies 284.5 and 286 eV. These correspond to the LUMO and LUMO+1 orbitals of the dye. The higher-lying peak near 287 eV in the difference spectrum lies close to the C−H σ^* orbital and is probably due to slightly different H coverages in the two top spectra. To ensure that the N atoms in the azide linker that attaches the dye to the diamond do not distort the result, a separate spectrum of a drop-cast sample of the linker is shown at the bottom of the figure. It contains a single π^* peak that partially fills the valley between the π^* peaks of the dye, without affecting their peak positions significantly. Least square fits to the π^* peaks of adsorbed and bulk dye show that any possible shift between them is smaller than ±0.02 eV, our detection limit. This shows that the covalent link to the diamond surface disturbs the electronic structure of the dye very little.

To determine the HOMO of the dye, a UPS spectrum of a diamond surface sensitized with $Ru(tpy)_2$ is shown in Figure 6a (top curve). It is compared to a similar spectrum of a H-terminated surface (dashed) via taking the difference (bottom curve, multiplied by a factor of 5), in the same way as for the NEXAFS spectra in Figure 5. In the difference spectrum a broad peak emerges at about 2.3 eV below the Fermi level. Moreover, by linear extrapolation of the bare diamond UPS data, the position of the VBM of diamond with respect to its Fermi level can be estimated. It is approximately 1.4 eV below the (surface) Fermi level, which is consistent with the result from NEXAFS and XPS in Figure 4b,c within the error bar of ±0.2 eV. Accordingly, the HOMO of the dye monolayer lies 0.9 eV below the VBM in Figure 6a. These energy differences have implications on the hole transport between the bulk diamond and the dye molecule, as discussed in a separate section below.

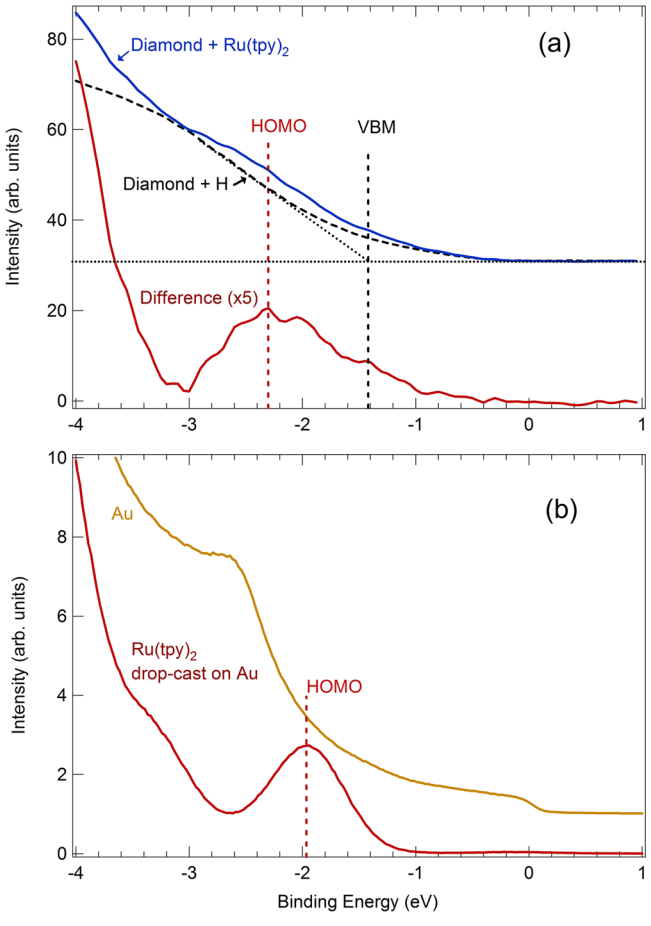

Figure 6. (a) Photoelectron spectra of diamond functionalized with $Ru(tpy)_2$ and H-terminated diamond at a photon energy of 50 eV. The difference spectrum represents the adsorbed dye. The linear extrapolation of the valence band edge yields an estimate of the VBM. The HOMO of the dye lies 0.9 eV below the VBM. (b) Photoelectron spectrum of a bulk $Ru(tpy)_2$ sample at a photon energy of 21.2 eV. All energies are relative to the Fermi level. A clean gold sample is used for energy calibration.

A comparison to the HOMO of the bulk dye can be made in Figure 6b, analogous to the comparison made for the LUMO in Figure 5. The bulk HOMO lies 2.0 eV below the Fermi level, close to the energy value determined for the dye monolayer. The bulk HOMO feature is significantly sharper than that of the dye attached to diamond. That could be due to multiple adsorption sites at the surface. Different radiation damage between the synchrotron and He(I) data could also play a role (compare the effect of irradiation on a phthalocyanine dye[35]).

Additional information on the position of the frontier orbitals of the $Ru(tpy)_2$ molecule was provided by UV−vis investigations carried out on an acetonitrile-based solution of the dye. The results, shown in Figure 7, reveal a peak in absorbance

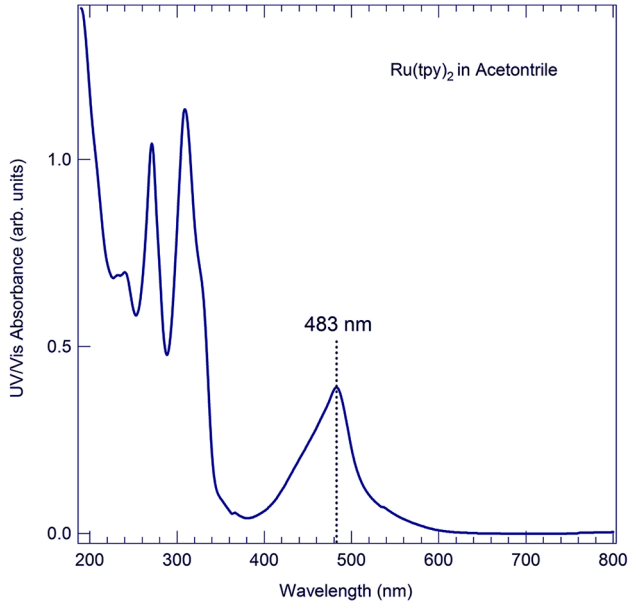

Figure 7. UV−vis absorption spectrum of a $Ru(tpy)_2$ solution in acetonitrile. The maximum absorbance is at a wavelength of 483 nm, which corresponds to a photon energy of 2.6 eV. This exciton energy value represents a lower limit for the HOMO−LUMO gap.

at wavelength 483 nm, which corresponds to a photon energy of 2.6 eV. This is the energy of an exciton between an electron in the LUMO and a hole in the HOMO, which is somewhat lower than the actual HOMO−LUMO gap (typically by a few tenths of an eV). No significant solvent effect on the band gap determination by UV−vis is expected.[36]

The excitonic energy shift in NEXAFS tends to be substantially larger than in UV−vis due to the stronger localization of the core excitation. To get a rough estimate of the excitonic shift at the C 1s edge, one can compare the

HOMO and LUMO obtained from NEXAFS and UV−vis with the true HOMO obtained from UPS. In the single-electron approximation, the NEXAFS spectra of Figure 5 show the LUMO of the $Ru(tpy)_2$ dye at 284.7 eV above the C 1s level. Subtracting the approximate HOMO−LUMO gap determined by UV−vis spectroscopy (2.6 eV), the HOMO of the dye comes out at 282.1 eV above the C 1s core level, that is, 1.7 eV below the VBM of diamond. This is to be compared with the actual position of the HOMO at 0.9 eV below the VBM from UPS. The difference of 0.8 eV between the two numbers can be ascribed mainly to the electron−hole interaction at the C 1s edge (neglecting electron−hole interaction in UV−vis spectroscopy). The attraction between the electron in the LUMO and the C 1s core hole shifts the NEXAFS transition to lower energy.

It is interesting to compare the electron−hole interaction at the C 1s and N 1s edges in metal−organic dyes containing a metal atom surrounded by π-bonded N atoms, such as $Ru(tpy)_2$ and porphyrins. The LUMO of these dyes tends to have strong weight on the N atoms. Therefore, one might expect a larger electron−hole interaction at the N 1s edge than at the C 1s edge. Indeed, a comparative study between theory and NEXAFS experiments of porphyrins finds an electron−hole interaction of about 3 eV for porphyrin dyes,[37] which is substantially larger than the C 1s electron−hole interaction we find here for $Ru(tpy)_2$. It would be quite useful to follow up on this comparison more systematically for extracting energy levels of dyes from NEXAFS.

IMPLICATIONS OF THE RESULTS ON SOLAR CELL DESIGN

Our spectroscopic results have implications on the use of dye-functionalized diamond surfaces as absorber−donor systems in solar cells or other solar energy conversion devices. Since the HOMO of the $Ru(tpy)_2$ molecule lies below the VBM of diamond, p-doped diamond could act as a donor in solar cells, refilling the hole created in the HOMO of the dye upon light excitation. However, our data suggest that the HOMO lies so low that a substantial voltage drop (of 0.9 V) would occur, with a corresponding reduction in the efficiency of the cell. That would not be an improvement over the tri-iodide electrolyte frequently used in DSSCs, where the voltage drop is typically 0.6 V.[38,39] To improve the device performance, dyes with a HOMO level higher than in $Ru(tpy)_2$, but still lower than the VBM of diamond, will have to be sought. Fine tuning of the HOMO may be achievable by attaching electron-donating groups, such as diphenylamino groups, to the pyridyl complex. A second improvement would be the reduction of the band gap of the molecules, optimizing it for the solar spectrum. The HOMO−LUMO gap of $Ru(tpy)_2$ is more than 1 eV larger than the optimum gap (1.4 eV) for a single-junction cell.[40] Molecules with larger π-systems have broader π and π^* bands and thereby narrower gaps. The smaller HOMO−LUMO gap of such molecules would not only provide more efficient solar light absorption but also reduce the HOMO-VBM offset and thus the voltage loss.

The results about the Fermi level pinning at the interface address a third bottleneck of solar cell performance, that is, the Schottky barrier between the donor and the dye. Although the VBM lies close to the Fermi level in the bulk of highly p-doped diamond, it drops to 1.4 eV below it at the interface to the dye molecules. That is a very large barrier compared to the width of the Fermi edge at room temperature (about 0.1 eV). It would require extreme doping levels to narrow the barrier enough to allow tunneling across it. In principle, the Schottky barrier can be modified by adsorbing polar molecules at the interface. Although this has been difficult in practice, it will be facilitated greatly by methods for attaching molecules to diamond covalently, such as the photochemical attachment used here for dye molecules.

CONCLUSIONS

In conclusion, the electronic properties of a B-doped diamond surface covalently sensitized with the organic dye $Ru(tpy)_2$ were spectroscopically investigated in comparison to a reference H-terminated surface. Bulk-sensitive fluorescence yield spectra reveal acceptor states in the band gap of diamond induced by the boron dopant. Surface-sensitive electron yield spectra of the attached dye help determine the energy of its LUMO, and photoemission studies reveal the position of its HOMO. The latter is found to lie 0.9 eV lower than the VBM of diamond. In a hypothetical solar cell using $Ru(tpy)_2$-sensitized diamond as a hole transport material, a fast refill of the hole in the dye can be expected, but the large voltage drop of 0.9 eV that drives the refill would lead to a large loss in efficiency. Possible dyes with a HOMO closer to the VBM would be organic molecules containing electron-donating groups and/or larger π-systems. The spectroscopic investigation of the electronic properties of such molecules can show the way toward higher solar energy conversion efficiencies via systematic energy level adjustment.

AUTHOR INFORMATION

Corresponding Author

*Tel.: 608-263-5590. Fax: 608-265-2334. E-mail: fhimpsel@wisc.edu.

Present Address

[▽]Natural Sciences Department, University of Wisconsin Superior, Superior, WI 54880, United States.

Notes

The authors declare no competing financial interest.

ACKNOWLEDGMENTS

This work was supported by the NSF with the awards CHE-1026245 and DMR-0537588 (SRC), by the DOE under the contracts DE-FG02-01ER45917 (end station) and DE-AC02-05CH11231 (ALS), by the Spanish Ministerio de Economia y Competitividad (MAT2010-21156-C03-01, C03-03, PIB2010US-00652), and by the Basque Government (IT-257-07). R.E.R. and R.J.H. acknowledge support from the NSF with grants CHE-0613010 and CHE-0911543.

REFERENCES

(1) Ruther, R. E.; Rigsby, M. L.; Gerken, J. B.; Hogendoorn, S. R.; Landis, E. C.; Stahl, S. S.; Hamers, R. J. *J. Am. Chem. Soc.* **2011**, *133*, 5692−5694.

(2) Yang, W.; Auciello, O.; Butler, J.; Cai, W.; Carlisle, J. A.; Gerbi, J. E.; Gruen, D. M.; Knickerbocker, T.; Lasseter, T. L.; Russell, J. N., Jr.; Smith, L. M.; Hamers, R. J. *Nat. Mater.* **2002**, *1*, 253−258.

(3) Strother, T.; Knickerbocker, T.; Russell, J. N., Jr.; Butler, J. E.; Smith, L. M.; Hamers, R. J. *Langmuir* **2002**, *18*, 968−971.

(4) Grätzel, M. *Nature* **2001**, *414*, 338.

(5) Cook, P. L.; Liu, X.; Yang, W.; Himpsel, F. J. *J. Chem. Phys.* **2009**, *131*, 194701.

(6) Preobrajenski, A. B.; Vinogradov, A. S.; Kleimenov, E.; Knop-Gericke, A.; Krasnikov, S. A.; Szargan, R.; Mårtensson, N. *Phys. Scr.* **2005**, *T115*, 1071−1073.
(7) Li, D.; Bancroft, G. M.; Fleet, M. E. *J. Electron Spectrosc. Relat. Phenom.* **1996**, *79*, 71−73.
(8) Jia, J. J.; Underwood, J. H.; Gullikson, E. M.; Callcott, T. A.; Perera, R. C. C. *J. Electron Spectrosc. Relat. Phenom.* **1996**, *80*, 509−512.
(9) Mele, E. J.; Ritsko, J. J. *Phys. Rev. Lett.* **1979**, *43*, 68−71.
(10) Ishizaka, K.; Eguchi, R.; Tsuda, S.; Chainani, A.; Yokoya, T.; Kiss, T.; Shimojima, T.; Togashi, T.; Watanabe, S.; Chen, C.-T.; Takano, Y.; Nagao, M.; Sakaguchi, I.; Takenouchi, T.; Kawarada, H.; Shin, S. *Phys. Rev. Lett.* **2008**, *100*, 166402.
(11) Himpsel, F. J.; Knapp, J. A.; VanVechten, J. A.; Eastman, D. E. *Phys. Rev. B* **1979**, *20*, 624.
(12) Pate, B. B. *Surf. Sci.* **1986**, *165*, 83−142.
(13) van der Weide, J.; Nemanich, R. J. *Appl. Phys. Lett.* **1993**, 1878−1880.
(14) Yang, W. L.; Fabbri, J. D.; Willey, T. M.; Lee, J. R. I.; Dahl, J. E.; Carlson, R. M. K.; Schreiner, P. R.; Fokin, A. A.; Tkachenko, B. A.; Fokina, N. A.; Meevasana, W.; Mannella, N.; Tanaka, K.; Zhou, X. J.; van Buuren, T.; Kelly, M. A.; Hussain, Z.; Melosh, N. A.; Shen, Z.-X. *Science (New York, N.Y.)* **2007**, *316*, 1460.
(15) Cui, J. B.; Ristein, J.; Stammler, M.; Janischowsky, K.; Kleber, G.; Ley, L. *Diamond Relat. Mater.* **2000**, *9*, 1143−1147.
(16) Morar, J. F.; Himpsel, F. J.; Hollinger, G.; Hughes, G.; Jordan, J. L. *Phys. Rev. Lett.* **1985**, *54*, 1960−1963.
(17) Morar, J. F.; Himpsel, F. J.; Hollinger, G.; Jordon, J. L.; Hughes, G.; McFeely, F. R. *Phys. Rev. B* **1986**, *33*, 1346.
(18) Batson, P. E. *Phys. Rev. Lett.* **1993**, *70*, 1822−1825.
(19) Gruen, D. M.; Krauss, A. R.; Zuiker, C. D.; Csencsits, R.; Terminello, L. J.; Carlisle, J. A.; Jimenez, I.; Sutherland, D. G. J.; Shuh, D. K.; Tong, W.; Himpsel, F. J. *Appl. Phys.* **1996**, *68*, 1640−1642.
(20) Birrell, J.; Gerbi, J. E.; Auciello, O.; Gibson, J. M.; Gruen, D. M.; Carlisle, J. A. *J. Appl. Phys.* **2003**, *93*, 5606.
(21) Bandis, C.; Pate, B. B. *Phys. Rev. Lett.* **1995**, *74*, 777−780.
(22) Nebel, C. E. *Semicond. Sci. Technol.* **2003**, *18*, S1.
(23) Bandis, C.; Pate, B. B. *Phys. Rev. B* **1995**, *52*, 12056.
(24) Diederich, L.; Küttel, O. M.; Aebi, P.; Schlapbach, L. *Surf. Sci.* **1998**, *418*, 219−239.
(25) Himpsel, F. J.; van der Veen, J. F.; Eastman, D. E. *Phys. Rev. B* **1980**, *22*, 1967−1971.
(26) Collins, A. T.; Williams, A. W. S. *J. Phys. C: Solid State Phys.* **1971**, *4*, 1789.
(27) Muramatsu, Y.; Takebe, T.; Sawamura, A. *X-Ray Spectrom.* **2007**, *36*, 162−166.
(28) Glans, P.-A.; Guo, J.-H. Private communication.
(29) Oguchi, T. *Sci. Technol. Adv. Mater.* **2006**, *7*, S67−S70.
(30) Hoffman, A.; Comtet, G.; Hellner, L.; Dujardin, G.; Petravic, M. *Appl. Phys.* **1998**, *73*, 1152−1154.
(31) Graupner, R.; Ristein, J.; Ley, L.; Jung, C. *Phys. Rev. B* **1999**, *60*, 23−29.
(32) Bobrov, K.; Comtet, G.; Dujardin, G.; Hellner, L.; Bergonzo, P.; Mer, C. *Phys. Rev. B* **2001**, *63*, 165421.
(33) Nakamura, J.; Yamada, N.; Kuroki, K.; Oguchi, T.; Okada, K.; Takano, Y.; Nagao, M.; Sakaguchi, I.; Takenouchi, T.; Kawarada, H.; Perera, R. C. C.; Ederer, D. L. *J. Phys. Soc. Jpn.* **2008**, *77*, 054711.
(34) Nakamura, J.; Kabasawa, E.; Yamada, N.; Einaga, Y.; Saito, D.; Isshiki, H.; Yugo, S.; Perera, R. C. C. *Phys. Rev. B* **2004**, *70*, 245111.
(35) Cook, P. L.; Johnson, P. S.; Liu, X.; Chin, A.-L.; Himpsel, F. J. *J. Chem. Phys.* **2009**, *131*, 214702.
(36) The bathochromic (red) shift of the UV−vis absorbance peaks corresponding to $\pi-\pi^*$ transitions due to solvent effects is very small, not larger than 5 nm. Any solvent-induced energy differences are within our energy resolution. See e.g.: Jakubikova, E.; Chen, W.; Dattelbaum, D. M.; Rein, F. N.; Rocha, R. C.; Martin, R. L.; Batista, E. R. *Inorg. Chem.* **2009**, *48*, 10720. Reichardt, C.; Welton, T. *Solvents and Solvent Effects in Organic Chemistry*; John Wiley and Sons: New York, 2011; pp 371−384.
(37) García-Lastra, J. M.; Cook, P. L.; Himpsel, F. J.; Rubio, A. *J. Chem. Phys.* **2010**, *133*, 151103.
(38) Grätzel, M. *Inorg. Chem.* **2005**, *44*, 6841−6851.
(39) Bessho, T.; Zakeeruddin, S. M.; Yeh, C.-Y.; Diau, E. W.-G.; Grätzel, M. *Angew. Chem.* **2010**, *122*, 6796−6799.
(40) Polman, A.; Atwater, H. A. *Nat. Mater.* **2012**, *11*, 174−177.